



ELSEVIER

Journal of Membrane Science 158 (1999) 187–209

Journal of
MEMBRANE
SCIENCE

A composite hollow fiber membrane-based pervaporation process for separation of VOCs from aqueous surfactant solutions

I. Abou-Nemeh¹, A. Das², A. Saraf³, K.K. Sirkar^{*}

*Department of Chemical Engineering, Chemistry and Environmental Science,
New Jersey Institute of Technology, Newark, NJ 07102, USA*

Received 28 July 1988; received in revised form 29 December 1998; accepted 29 December 1998

Abstract

The separation and recovery of VOCs from surfactant-containing aqueous solutions by a composite hollow fiber membrane-based pervaporation process has been studied. The process employed hydrophobic microporous polypropylene hollow fibers having a thin plasma polymerized silicone (PDMS) coating on the outside diameter, trichloroethylene (TCE) as the model contaminant and sodium dodecyl sulfate (SDS) as the surfactant. The feed solution was passed through the fiber bore; the shell side had vacuum. The process operating parameters, e.g., feed flow rate, TCE and SDS concentrations, were varied over a wide range to investigate their effect on the process performance. Depending on the concentration of the surfactant, separation of VOCs can be achieved via two different conditions, namely, wetted pore and non-wetted pore. The resistances-in-series concept successfully applied earlier to the TCE–water system has been extended to the TCE–SDS–water system for both wetted pore and non-wetted pore conditions. Results will be provided also for a more complex feed solution containing alcohols and the hydrophilic polymer, xanthan gum. © 1999 Elsevier Science B.V. All rights reserved.

Keywords: Pervaporation; Plasma polymerized membranes; Fiber membranes; Volatile organic compounds; Surfactants

1. Introduction

Groundwater and aquifer contamination frequently consists of light non-aqueous phase liquids (LNAPLs), e.g., benzene, toluene or other polyaromatic hydrocarbons (PAHs) and dense non-aqueous phase liquids (DNAPLs), e.g., TCE. Limitations of conventional pump-and-treat remediation, initially prescribed as the method to clean-up such subsurface organic con-

taminations, have been well recognized [1]. New technologies are being developed to mobilize and solubilize the so-called “pockets” of LNAPLs and DNAPLs and boost their removal efficiency. Of these, surfactant flushing is being increasingly recognized as an efficient method for recovering residual LNAPLs and DNAPLs from contaminated groundwater [2–4]. Fountain et al. [5] successfully demonstrated surfactant enhanced remediation of DNAPLs at two different sites.

Such a process results in large volumes of over-ground surfactant-flushed water rich in VOCs, LNAPLs, DNAPLs, oils, surfactants, dissolved salts, alcohols and polymers. This has to be treated to remove VOCs before discharge or reuse. Several technologies, e.g., air and steam stripping, carbon

^{*}Corresponding author. Tel.: +1-973-596 8447; fax: +1-973-596 8436; e-mail: sirkar@admin.njit.edu

¹Present address: Roquette America, Keokuk, IA, USA.

²Present address: Cyberstaff America Ltd., New York, NY, USA.

³Present address: Alpha Metals Inc., New Jersey, NJ, USA.

adsorption, solvent extraction, etc., for groundwater treatment and VOC separation for on-site remediation have been proposed [6]. These traditional technologies have many shortcomings. An alternative method is the pervaporation (PV) process. The superiority of PV over others can be characterized by volume reduction, concentration and recovery of contaminants, surfactant recycling and reuse after preconcentration, compactness, easy design and scale-up and possible cost effectiveness.

Laboratory studies of pervaporation-based recovery of VOCs like 1,1,1-trichloroethane (TCA) from a surfactant-containing solution have been carried out using flat 127 μm thick silicone rubber membrane [7]. When micellar solutions were utilized, pervaporation was capable of removing the VOC from the solution, even as the micelles significantly reduced the extracellular concentration of TCA and therefore the pervaporation performance. Based on these good performances, pilot studies were conducted by these investigators [8]. Using 5000 gal of VOC-laden surfactant solution (from Hill Air Force Base, Ogden, UT), pervaporation-based removal of VOCs was carried out in a pilot plant (EPA, T & E Facility, Cincinnati, OH) having spiral-wound pervaporation modules at feed flow rates between 0.25 and 2 gpm. This pilot-scale study encountered one major difficulty, namely, an unusual and considerable increase in the feed solution pressure drop which vitiated the otherwise excellent pervaporation performance vis-à-vis VOC removal. Apparently, residual heavy oils in the extracted surfactant-flushed water fouled the flow channels of the spiral-wound units badly.

We had initiated sometime back a hollow fiber membrane-based study of removal of VOCs from surfactant-containing solutions via a modified pervaporation process. This study was specifically designed to handle VOCs as well as heavy oils. In fact, pilot plant studies carried out at the EPA pilot plant (Cincinnati, OH) using the same batch of recovered surfactant-flushed water (available in a 5000 gal tanker) through 2 in. diameter hollow fiber membrane modules did not encounter any pressure drop or fouling problems over an extended period of testing [9]. These results will be communicated later [10]. We focus here on a fundamental study to explore the hollow fiber membrane-based modified pervaporation process for surfactant-containing feeds.

The hollow fibers are made of hydrophobic microporous polypropylene; a thin non-porous layer of silicone membrane is plasmopolymerized on the outside surface. The aqueous solution is made to flow through the fiber bore where it encounters the pores of the hydrophobic substrate. A vacuum is pulled from the shell side; the silicone coating being strongly bonded to the substrate does not get stripped off in this mode of operation. When the aqueous solution does not have any surfactants, it does not wet the pores. The VOCs are stripped from the solution into the gas-filled pores where they undergo vapor permeation-based removal through the silicone membrane to the shell side. This is unlike ordinary pervaporation where the aqueous solution is imposed directly on the silicone rubber membrane. We call it "stripmeation". We have characterized the various resistances encountered by the VOC in this process and successfully described the observed behavior [11]. The feed flow inside fibers with an outside membrane layer has been justified in [11] for cases where there would be heavy oil in the feed. If the membrane layer was on the fiber ID, the permeated oil in the pore would have caused very high permeate side pressure drop. In the mode adopted, the oil would accumulate in the pore and then will be permeated to the shell side where the open space will not provide any resistance to pulling a vacuum for pervaporation removal of VOC.

We explore here the behavior of the process when there are surfactants in the aqueous solution. The surfactant is sodium dodecyl sulfate (SDS); the VOC is trichloroethylene (TCE). The surfactant concentration has been varied between 0.3% and 3%; the TCE concentration was varied between 200 and 3500 ppm. In a few cases, a far more complex feed solution was employed to simulate the type of solutions likely to be extracted from an actual surfactant flushing process. The module performances in terms of TCE removal, TCE flux and water flux have been determined. The behavior of the mass transfer coefficient has been analyzed in terms of the various resistances in series encountered in TCE transport. The objectives here are to study the process parameters and evaluate its feasibility for the treatment of surfactant-flushed water streams. The effects of the surfactant (SDS) and contaminant (TCE) concentrations, temperature and hydrodynamics have been studied. The resistances-in-series model developed earlier [11] has been adopted and modified.

2. Resistances-in-series description for the overall mass transfer coefficient

When a surfactant-containing aqueous solution of TCE flows in the bore of a hydrophobic microporous hollow fiber having a non-porous silicone coating on the fiber outer diameter, a number of scenarios are possible. If the solution surface tension is equal to or less than the critical surface tension of the hydrophobic substrate, then the solution will spontaneously wet the pores of the substrate. When the pores are wetted, free monomeric surfactant as well as micelles of the feed solution will be present in the pores. This solution will then be imposed on the silicone membrane coating and pervaporation of TCE will occur through the

silicone membrane. There is considerable possibility of adsorption of at least a monomolecular layer of surfactants on the hydrophobic pore surface under such conditions.

If the surface tension of the solution happens to be higher than the critical surface tension of the hydrophobic substrate, the solution will not spontaneously wet the pores; the pores will remain filled with gas. Under such a condition, TCE will be stripped from the solution into the gas-filled pore and then undergo removal through the silicone membrane by vapor permeation after diffusion through the gas-filled pore. The situation would correspond to that in “stripmeation” described in [11]. We show these two situations in Fig. 1(A) and Fig. 2(A); Fig. 1(A) is for wetted

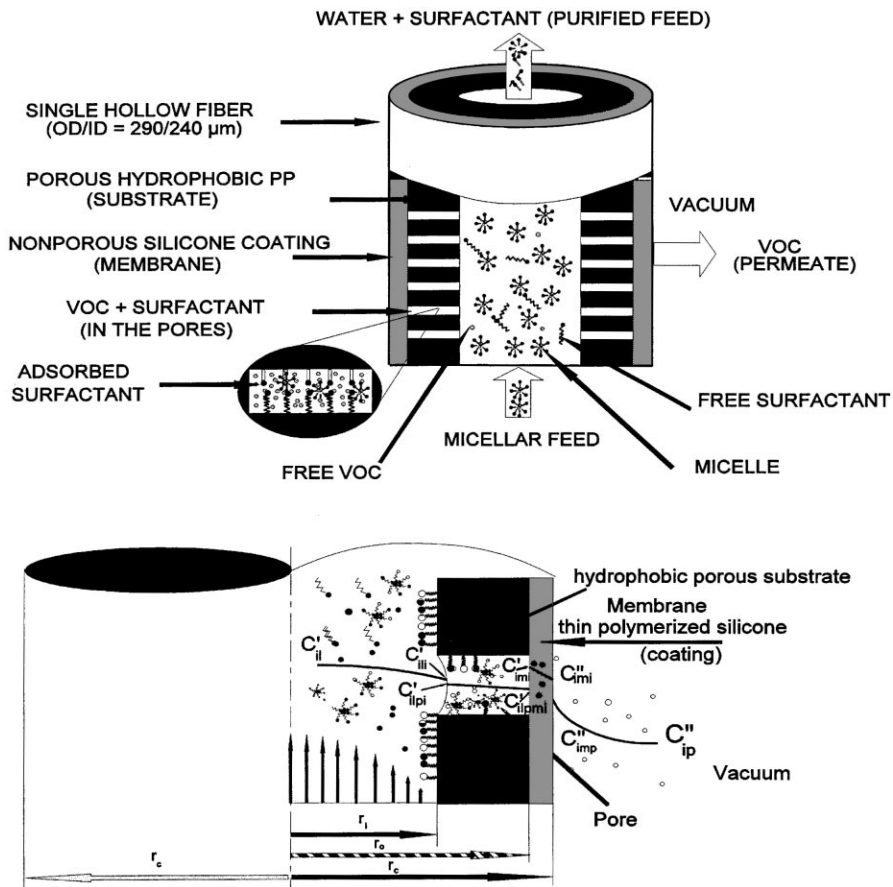


Fig. 1. (A) A schematic diagram of a hollow fiber in pervaporation with tube-side feed of VOC in a micellar feed. (B) The concentration profile of a VOC in a hollow fiber membrane-based modified pervaporation process with water-filled pore (wetted pore case).

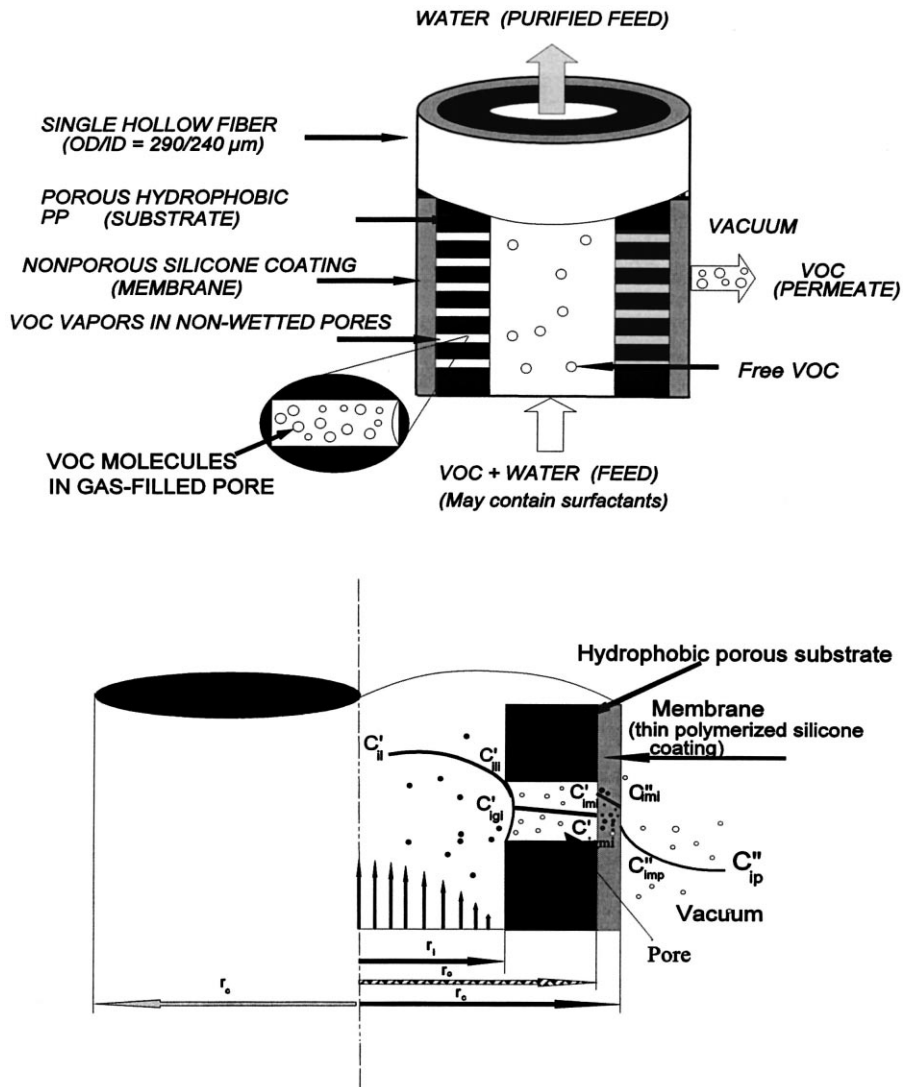


Fig. 2. (A) A schematic diagram of a hollow fiber in pervaporation with tube-side feed of VOC in water for non-wetted pores. (B) The concentration profile of a VOC in a hollow fiber membrane-based modified pervaporation process with gas-filled pore (non-wetted pore).

pores and Fig. 2(A) is for gas-filled pores. The TCE concentration profiles are shown in Fig. 1(B) and Fig. 2(B), respectively.

There are four resistances to TCE transport in either case. They are: (1) feed boundary layer resistance in the fiber bore; (2) transport resistance through the pore; (3) transport resistance through the silicone membrane; (4) transport resistance in the vacuum-side boundary layer. Das et al. [11] have shown that the vacuum-side boundary layer resistance could be

neglected in their case. It should be no different here since other resistances are increased in the presence of surfactants. The overall mass transfer coefficient, K_o , for TCE (species i) transport is defined by the expression for the molar rate of transfer of species i per unit fiber length, R_i ,

$$R_i = K_o \pi d_o (C'_{il} - C''_{ipl}), \quad (1)$$

where C''_{ipl} is a hypothetical liquid phase concentration in equilibrium with the vacuum-side gas phase con-

centration C''_{ip} and is related by the equilibrium relation Eq. (2a) below. To relate K_o to the other individual mass transfer coefficients, we first define the following partition coefficients:

1. Non-wetted pore (Fig. 2(A)):

$$\text{Liquid-gas : } C'_{li} = H_{ig} C'_{igi} \quad (2a)$$

$$\text{Gas-membrane : } C'_{imi} = m_{vf} C'_{igmi} \quad (2b)$$

$$\text{Membrane-vacuum : } C''_{imp} = m_{vp} C''_{imi} \quad (2c)$$

2. Wetted pore (Fig. 1(A)):

$$\text{Liquid-liquid : } C'_{li} = H_{il} C'_{ilpi} \quad (3a)$$

$$\text{Liquid-membrane : } C'_{imi} = m_{lf} C'_{ilpmi} \quad (3b)$$

$$\text{Membrane-vacuum : } C''_{imp} = m_{vp} C''_{imi} \quad (3c)$$

For non-wetted pores, the individual mass transfer coefficients are defined by the following relations:

$$\text{Aqueous boundary layer : } R_i = k_1^f \pi d_i (C'_{il} - C'_{li}) \quad (4)$$

$$\text{Gas filled pore : } R_i = k_{gp}^f \pi d_{lm} (C'_{igi} - C'_{igmi}) \quad (5)$$

$$\text{Silicone membrane : } R_i = k_m \pi d_o (C'_{imi} - C''_{imi}) \quad (6)$$

The relation between the overall mass transfer coefficient, K_o , and the individual coefficients in Eqs. (4)–(6) [11] is

$$\frac{1}{K_o} = \frac{d_o}{k_1^f d_i} + \frac{H_{ig} d_o}{k_{gp}^f d_{lm}} + \frac{H_{ig}}{m_{vf} k_m} \quad (7)$$

For wetted pores, the individual mass transfer coefficients are defined by the following relations:

$$\text{Aqueous boundary layer : } R_i = k_1^f \pi d_i (C'_{il} - C'_{li}) \quad (8)$$

$$\text{Liquid filled pore : } R_i = k_{lp}^f \pi d_{lm} (C'_{ilpi} - C'_{ilpmi}) \quad (9)$$

$$\text{Silicone membrane : } R_i = k_m \pi d_o (C'_{imi} - C''_{imi}) \quad (10)$$

$$\text{Vacuum boundary layer : } R_i = k_g^p \pi d_o (C''_{imp} - C''_{ip}) \quad (11)$$

We will neglect the vacuum side boundary layer

resistance. The relation between K_o and the individual coefficients in Eqs. (8)–(10) is obtained as

$$\frac{1}{K_o} = \frac{d_o}{k_1^f d_i} + \frac{H_{il} d_o}{k_{lp}^f d_{lm}} + \frac{H_{il}}{m_{lf} k_m} \quad (12)$$

In the wetted pore case, C'_{ilpi} is the pore phase concentration of species i in the wetted pore at the feed solution-membrane pore interface and is in equilibrium with C'_{li} , the feed liquid concentration at the pore mouth via Eq. (3a). Normally, the quantity H_{il} should have a value 1 with a wetted pore unless the pore causes some degree of partitioning between the feed liquid and the pore liquid. Similarly, there is a possibility of an additional resistance due to the surfactants being present at the gas-liquid interface at the pore mouth for non-wetted pores.

From the detailed studies by Das et al. [11], the resistance of the gas-filled pore was found to be negligible compared to the boundary layer resistance ($d_o/k_1^f d_i$) and the silicone membrane resistance ($H_{ig}/m_{vf} k_m$). Thus, for a gas-filled non-wetted pore, Eq. (7) is reduced to

$$\frac{1}{K_o} = \frac{d_o}{k_1^f d_i} + \frac{H_{ig}}{m_{vf} k_m} \quad (13)$$

In the studies by Das et al. [11], estimates of k_1^f for the tube-side boundary layer was obtained from Graetz solution since the feed was merely an aqueous solution of TCE. The presence of surfactant as micelles here would not allow an a priori prediction of the k_1^f from Graetz solution since the kinetics of breakage of the micelles with the membrane wall is not known. Ordinary convective diffusion is influenced here by two additional effects: (1) a reduction in the concentration of free TCE due to micellar solubilization; and (2) release of TCE from the micelle due to rupturing of the micelles after collision with the walls. An additional unknown is: is the pore wetted or not. This question may be answered by comparing the performance of the system having deliberately wetted pores and that without deliberately wetted pores.

For wetted pores, the pore-based diffusional resistance cannot be neglected in Eq. (12). It may be estimated using the notion of diffusion of species i in the tortuous pores:

$$k_{lp}^f = \frac{D_{il} \epsilon_m}{\tau_m \delta_m} \quad (14)$$

This does not consider any effect due to the presence of micelles as well as any adsorbed layer in the pore wall.

3. Experimental

3.1. Chemicals and materials

Trichloroethylene (TCE, purity 99.9%, density 1.456 g/cm³ and FW 131.39), acetonitrile (HPLC grade purity 99.9%) and isopropyl alcohol (IPA, HPLC grade) were from Fisher Scientific (Springfield, NJ). Sodium dodecyl sulfate (SDS, purity 99%, FW 288.4) and hydrophilic polymer xanthan gum (practical grade) were from Sigma (St. Louis, MO). Ultra-pure N₂, He, air-zero and liquid CO₂ were from Matheson (E. Rutherford, NJ).

3.2. Hollow fiber membrane module

The general characteristics of the hollow fibers are as follows. The composite fiber consists of a hydrophobic hollow fiber support having a plasma polymerized thin non-porous silicone skin on the outer surface. The substrate (support) is polypropylene Celgard X-10[®] (Hoechst Celanese, Charlotte, NC). The characteristics of the module used are given in Table 1. Details of fabrication of the module are provided in [12].

3.3. Experimental unit

The experimental unit used is shown in Fig. 3. The feed solution which was freshly prepared from stock SDS-solution was pumped into the hollow fiber membrane module by a peristaltic Masterflex pump having a digital console drive Model 7523-20 (Cole-Parmer,

Vernon Hills, IL) from a collapsible Teflon bag (Cole-Parmer, Vernon Hills, IL). Different sizes of bags were used depending on the flow rate and the duration of the run. Teflon tubing of 1/4 in. ID (Cole-Parmer, Vernon Hills, IL) and stainless steel fittings (Swagelok, R.S. Crum, New Brunswick, NJ) were used for the feed and all connecting lines from the feed reservoir to and from the membrane module. A micrometering valve (Swagelok, R.S. Crum, New Brunswick, NJ) was installed at the outlet feed line to regulate feed back-pressure. An oilless vacuum pump (Model UN 726.112 FTP KNF-Neuberger, Trenton, NJ) was used to evacuate and maintain a permeate-side vacuum of 20–25 Torr. The permeate pressure was controlled by a Digital Vacuum Regulator (DVR) Model 2000 (J-Kem Scientific, St. Louis, MO). For the low pressure lines, convoluted Teflon tubing (Cole-Parmer, Vernon Hills, IL) was used to connect the condensers with module and the evacuating system. For tuning and adjusting the set vacuum, an additional micrometer vacuum valve (McMaster Carr, Dayton, NJ) was installed between the DVR and the vacuum pump. The module was immersed in a water bath interfaced to a thermostat (Fisher Scientific, Springfield, NJ) to maintain a constant temperature. Two condensers specially designed were connected in parallel and used to collect the permeate during steady state and non-steady state conditions. A mixture of dry ice and methanol was used as the cooling medium in a Dewar flask (Labglass, Vineland, NJ) inside which each condenser was kept to trap the permeate vapor from the module outlet.

3.4. Analytical procedure

Two techniques were used to measure the TCE concentration in aqueous samples: high pressure liquid chromatography (HPLC); headspace gas

Table 1
Characteristics of the module used

Module no.	Fiber substrate	Membrane coating	No. of fibers	OD (μm)	ID (μm)	Active length (cm)	Mass transfer area based on OD (cm ²)	Remarks
1	Celgard X-10 ^{®a}	Silicone ^b	75	290	240	20.5	140.1	Fabricated in lab

^a Porosity (ϵ_m) is 0.4 and tortuosity (τ_m) is 2.49 [28].

^b Plasma polymerized by AMT, Minnetonka, MN.

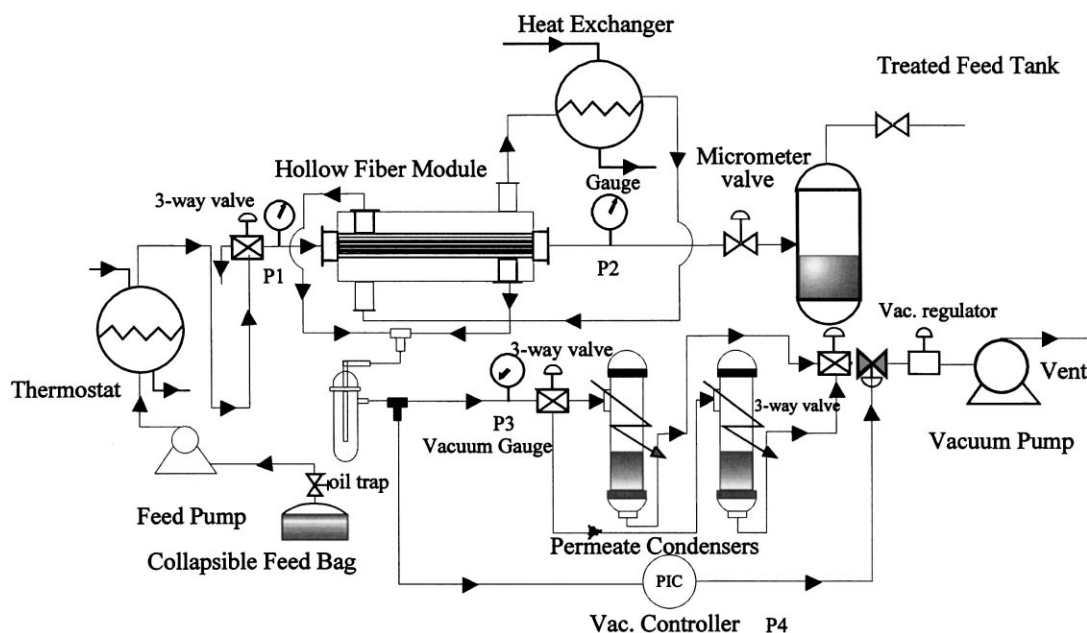


Fig. 3. A schematic diagram of the pervaporation experimental unit.

chromatography (HSGC). For quality assurance and quality control (QA/QC) purposes, the combination of both were used. Highlights of both methods will be mentioned here; details can be found in [12].

3.4.1. High pressure liquid chromatography

Aqueous TCE concentration was measured in a HP series II 1090 HPLC with a HP 3390 integrator and an autosampler (Hewlett Packard, Wilmington, DE). A reverse-phase Hypersil[®] ODS C18 HP column (5 μm , 100 \times 4.6 mm, Hewlett Packard, Wilmington, DE) was used. An AltGuard system (Alltech, Deerfield, IL) was used with Hypersil[®] ODS C18 HP column 5 μm Alltech guard column to protect the column from any damage and contamination. The mobile phase was 60% acetonitrile and 40% deionized and filtered water. TCE concentration was determined using an injection volume of 5 μl at 200 nm wavelength (UV detector) and a mobile phase flow rate of 0.4 ml/min. The HPLC was calibrated for TCE concentration ranging from 0 to 120 ppm for TCE–water standards. The response was linear. Analogous standards were prepared also with TCE in SDS–water standards for 0.3%, 1.0%, 3.0% and 5% (w/v) SDS. The UV detector response for both TCE–water as well as

TCE–SDS–water were nearly identical. For every sample analyzed, two injections were made; the average was taken as the actual response.

3.4.2. Headspace gas chromatography

Aqueous TCE sample concentration was also measured by the HSGC containing an HP 6890 series gas chromatograph using a HP 7694 headspace sampler and HP 6890 series integrator (Hewlett Packard, Wilmington, DE). TCE was analyzed by a flame ionization detector (FID) using HP-5 capillary column (crosslinked 5% PH ME siloxane) of 30 m length, 320 μm diameter and 1 μm film thickness (Hewlett Packard, Wilmington, DE). The carrier used was ultrapure nitrogen. Analysis of TCE-containing aqueous solutions of varying surfactant concentrations posed difficulties in reproducing results using the direct liquid injection headspace technique because of their sensitivity to matrix variation. It also required proper calibration curves for each sample matrix. This was extremely difficult as the compositions of the samples varied widely or were unknown. The methodology of full evaporation technique (FET) was used to overcome the matrix effects [13]. This technique is based on a near-complete transfer of analytes from the

condensed matrix into a vapor phase. This transfer eliminated the possibility of contamination from any non-volatile component in the sample such as SDS; also the sample integrity was not affected by the matrix. From thermodynamic estimation it was found that a 13 μl of sample in a 22.5 ml headspace vial was needed to achieve full evaporation. The optimal parameters of the headspace sampler were as follows: oven temperature 100°C, sample equilibration time 7 min, pressurizing time 0.15 min, sampling time 1 min. An optimal temperature program for the GC was followed to obtain a clear separation of TCE. The initial oven temperature was set at 40°C for 1.5 min followed by temperature ramping at 25°C/min until it reached 75°C where it was kept for 1 min. In the final step, the temperature was ramped at 40°C/min until 160°C which was maintained for 3 min to purge the column of any residues.

3.5. Experimental procedure

The feed solution was prepared by adding appropriate amount of TCE to the SDS–water stock solution prepared at least 48 h before the experiment for proper micelle formation. The feed thus prepared was pumped into the Teflon collapsible bag to prevent the formation of headspace during an experimental run and keep the feed concentration nearly constant. The feed was kept at a pressure 5–7 psig by using a micrometer control valve (Swagelok, R.S. Crum, New Brunswick, NJ) in the retentate line. The feed pressure was monitored using a dial pressure gauge. Dewar flasks were filled with dry ice and methanol after putting in the condensers. The experiment was started by pumping the feed into the module; after 3 h, a steady state was reached. Usually one run lasted for 6–8 h. Samples were withdrawn every half-an-hour and analyzed for VOC content. The experiment was stopped once consistent results were obtained from 4 to 6 consecutive samples. The permeate was measured gravimetrically. The method relied on weighing the condenser before and after the experiment and the difference was the amount of water and TCE collected. The amount of pure water permeate was estimated after analyzing the permeate for TCE content. When the concentration of TCE in the permeate is above the solubility limit in water, two phases are formed; the organic phase can then be easily decanted from the aqueous phase and its volume noted.

3.6. Wetted pore experiments

The experimental procedure followed for wetted pore experiments was similar to that for regular pervaporation experiments, except that the pores of the hollow fiber membrane were wetted prior to starting the experiment. The technique used to wet the pores was adopted from Bhawe and Sirkar [14]:

1. Pass an aqueous solution of ethyl alcohol (40%, v/v) on the tube side of the hollow fiber membrane module at a flow rate of 0.6 ml/min for a period of 3 h.
2. Pass pure water on the tube side of module at a flow rate of 0.6 ml/min for a period of 3 h.
3. Repeat step 2.

It is assumed that by following the above procedure, water will be immobilized within the pores for the entire thickness of the support [14]. Such a film is considered fully exchanged and is referred to as immobilized water membrane (IWM). After the pores are wetted following the procedure mentioned above, pervaporation run is carried out with TCE–water or SDS–TCE–water system.

3.7. Calculated quantities

Percent removal of TCE is defined as

$$\% \text{ Removal} = \frac{C_{\text{inlet}} - C_{\text{outlet}}}{C_{\text{inlet}}} \times 100 \quad (15)$$

The fluxes of TCE and water were obtained, respectively, from the volumes of the TCE phase and water phase collected over time t from the membrane of area A_m :

$$J_i = \frac{V_{\text{TCE}} \rho_{\text{TCE}}}{A_m t} \quad (16)$$

$$J_w = \frac{V_{\text{H}_2\text{O}} \rho_{\text{H}_2\text{O}}}{A_m t} \quad (17)$$

where J_i and J_w are TCE flux and water flux, respectively.

Here A_m is defined as

$$A_m = \pi d_o N L \quad (18)$$

where N is the number of hollow fibers of outside diameter d_o and length L . The Reynolds number for

flow inside the fiber for water (as well as SDS solutions used) is defined by

$$Re = \frac{d_i \rho_{H_2O} \nu}{\mu_{H_2O}} \quad (19)$$

The viscosities and densities of SDS solutions were essentially very close to that of water. Here the velocity of the solution ν for a volumetric flow rate of Q ml/min is obtained from

$$\nu = \frac{4Q}{60N\pi d_i^2} \quad (20)$$

The overall mass transfer coefficient K_o for TCE is obtained from

$$J_i = K_o \Delta C_{lm} \quad (21)$$

where ΔC_{lm} is obtained from (22) assuming $C_{inlet}^p \ll C_{inlet}$ and $C_{outlet}^p \ll C_{outlet}$ for calculating K_o :

$$\Delta C_{lm} = \frac{(C_{inlet} - C_{inlet}^p) - (C_{outlet} - C_{outlet}^p)}{\ln[(C_{inlet} - C_{inlet}^p)/(C_{outlet} - C_{outlet}^p)]} \quad (22)$$

4. Results and discussion

4.1. The effect of SDS on the removal of VOC

Three SDS concentrations, i.e., 0.3%, 1.0% and 3% were extensively employed with TCE concentrations varying from 200 to 3500 ppm. The feed flow rate to

the module was 2.5 ml/min; the applied vacuum was 20 Torr. The results of TCE removal versus its feed concentration for different SDS levels are shown in Fig. 4. The module behavior for a TCE–water solution without any surfactants is also shown for comparison [11]. As can be seen for the TCE–water system (no SDS), a 93–96% removal was achieved irrespective of the initial TCE concentration. The range of TCE concentrations used was limited to its maximum solubility in the aqueous phase, i.e., 900–1000 ppm [15]. The addition of SDS to the TCE–water system enhances the apparent solubility of the TCE in the aqueous solutions via micellar solubilization. For SDS–TCE–water systems, the removal of TCE dropped from 95% to 89% for 0.3% SDS (which is just above the CMC ($CMC_{SDS}=0.24\%$)). Further addition of SDS caused a drop in the removal from 89% to 67% and 37% for 1% and 3% SDS, respectively.

4.2. The effect of SDS on TCE flux

In Fig. 5 the flux of TCE has been plotted versus the feed TCE concentration. Essentially, a straight line was obtained for each system irrespective of the SDS content. The reduction in TCE removal observed earlier on SDS addition to the TCE–water system was also observed here. The flux of TCE was reduced by 2.3%, 29.6% and 43.3% for 0.3%, 1% and 3% SDS systems, respectively. One possible explanation for the

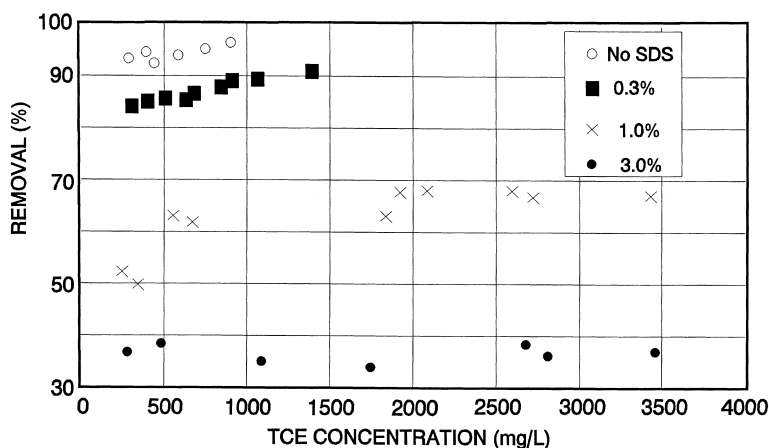


Fig. 4. The effect of TCE concentration on TCE removal for different SDS concentrations (temperature=25°C; vacuum=20 Torr; flow rate=2.5 ml/min; TCE=270–3500 ppm).

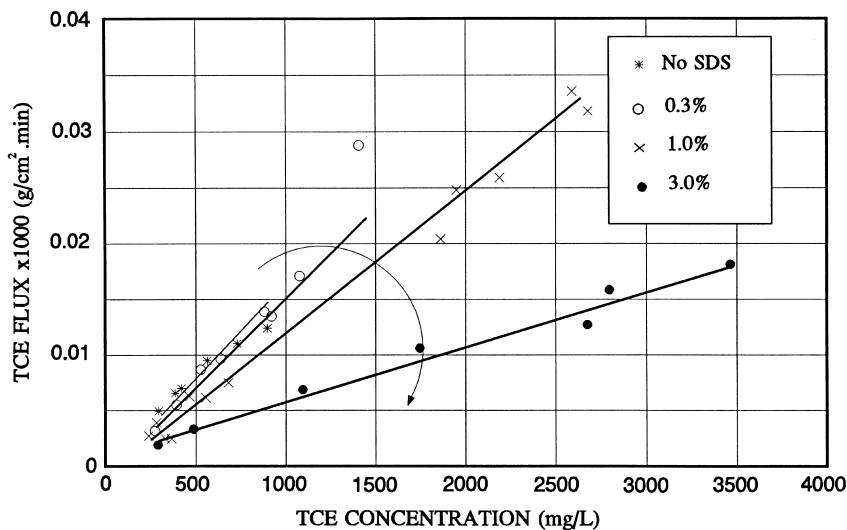


Fig. 5. The effect of TCE concentration on the flux for different SDS concentrations (temperature=25°C; vacuum=20 Torr; flow rate=2.5 ml/min; TCE=270–3500 ppm).

flux reduction is the dilution effect of the TCE–water system by SDS. With increasing concentration of SDS, the number of micelles as well as the aggregation number of micelles increase [16]. This results in a dilution of the solubilize (TCE), which was kept constant for every SDS–TCE–water system studied. It is also known that the higher the concentration of the surfactant, the higher the aggregation number and in the presence of an electrolyte in the system it may reach 100–1000. This will result in a longer residence time needed for the micelles to dissociate and release their load. Equally a smaller amount of TCE will be released when a micelle is dissociated. Conversely, the number of micelles increase substantially; however, the net effect must be a reduction in the net rate of TCE release for removal through the membrane. There must also be an additional resistance to TCE transport provided by the monolayer of adsorbed surfactants on the silicone membrane surface for wetted pore conditions.

4.3. The effect of SDS on the mass transfer coefficient

The overall mass transfer coefficient for TCE estimated according to Eq. (21) has been plotted against the TCE concentration for three SDS concentrations in Fig. 6. The feed flow rate was 2.5 ml/min (the corre-

sponding Reynolds number is about 3). For the TCE–water system the mass transfer coefficient is almost unaffected by the variation of TCE in the feed and is equal to 8.5×10^{-4} cm/s. However, when SDS was added to TCE–water system, a drop in the mass transfer coefficient was observed. A marginal drop was observed for the 0.3% SDS–TCE–water system. Considerable drop was observed for the 1% and 3% SDS–TCE–water systems. No effect of TCE concentration on mass transfer coefficient was noticed for two SDS concentrations 1% and 3%.

4.4. The effect of feed hydrodynamics

4.4.1. TCE mass transfer coefficient

A vast majority of the reported investigations on mass transport in pervaporation indicate that diffusional resistance of the membrane as well as the thin feed boundary layer essentially control the permeation flux and interfacial equilibrium prevails on both upstream and downstream sides. The boundary layer diffusional resistance can even control the overall transport process. We have seen in Part I of this study [11] on removal of traces (800–900 ppm) of TCE from water (no SDS) and from the resistances-in-series model that the diffusional resistance for transport across the PDMS membrane was about one order lower than that for the tube-side feed mass transfer

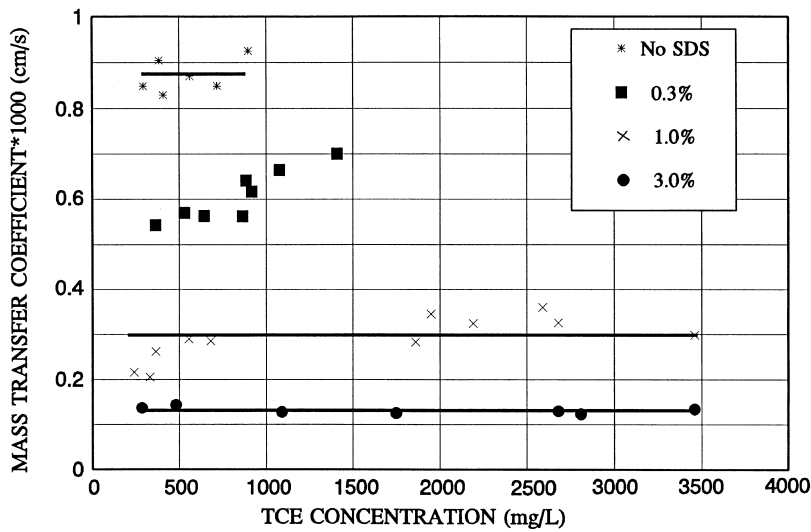


Fig. 6. The effect of TCE concentration on TCE mass transfer coefficient (temperature=25°C; vacuum=20 Torr; flow rate=2.5 ml/min; TCE=270–3500 ppm).

resistance over the investigated range of Reynolds number from 3 to 180. Therefore, the overall mass transfer resistance is primarily controlled by the liquid feed boundary layer.

The values of TCE mass transfer coefficient versus Reynolds number have been plotted in Fig. 7. The values for the TCE–water system [11] are also shown

in the same figure. As the Reynolds number was increased from 3 to 200, the overall TCE mass transfer coefficient was increased significantly; for 1% SDS solution, the increase was from 3.5×10^{-4} to 6.5×10^{-4} cm/s. For this system, overall mass transfer coefficient kept on increasing with the increase in Reynolds number. However, for the 0.3% SDS solu-

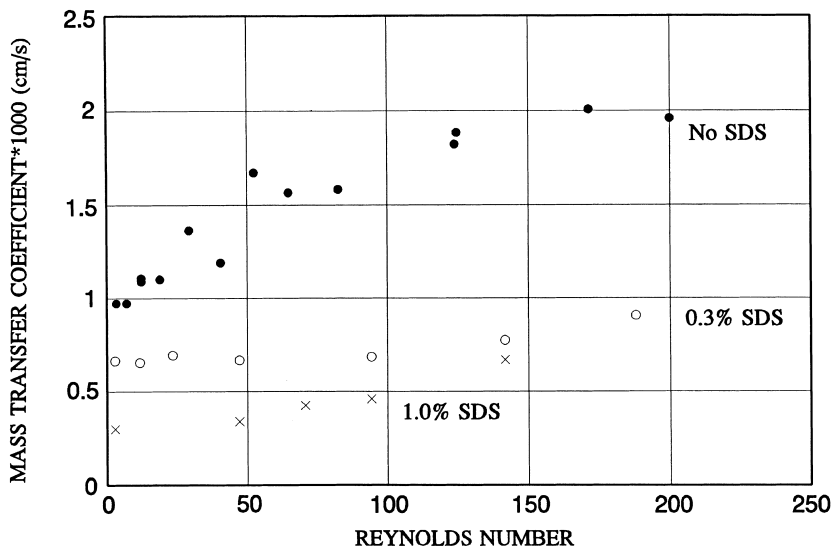


Fig. 7. Effect of hydrodynamics on TCE mass transfer coefficient (temperature=25°C; vacuum=20 Torr; TCE=700–3500 ppm; feed-bleed mode).

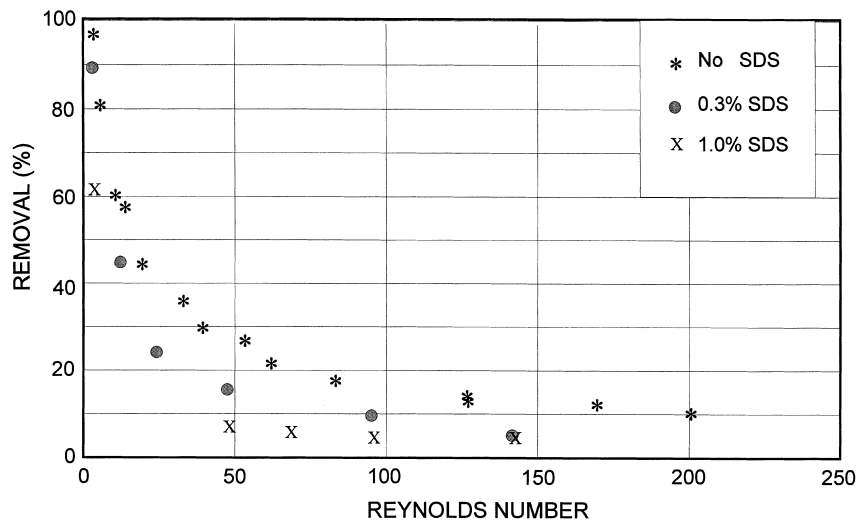


Fig. 8. Effect of hydrodynamics on TCE removal (temperature=25°C; vacuum=20 Torr; TCE=700–3500 ppm; feed-bleed mode).

tion such a trend can be observed only beyond $Re=140$.

4.4.2. The removal of TCE

To understand better the impact of SDS on mass transfer, we studied the effect of the feed flow rate on TCE removal, its flux and water flux. The results of TCE removal are shown in Fig. 8. The feed flow rate was varied from 2.5 to 160 ml/min. TCE feed concentration was constant for a given SDS concentration. The removal of TCE decreased exponentially with increasing feed flow rate for all SDS-containing systems. The removal dropped from 89% to 5% for 0.3% SDS system upon increasing the flow rate from 2.5 to 80 ml/min; any further increase in the flow rate did not affect substantially the removal reaching a stable value of about 5%. For the SDS-systems the removal profile was almost identical to that for the TCE–water system; the higher the SDS concentration the lower the removal with a tendency of levelling off at higher Reynolds numbers, i.e., from 50 to 150 reaching a value of 12% and 5% for 0.3% and 1% SDS–TCE–water systems, respectively. This result was due to a drastic reduction in residence time due to the increased flow rate.

4.4.3. TCE flux

The behavior of TCE flux is rather interesting; a non-linear characteristic was obtained for the flux

versus the feed flow rate as shown in Fig. 9. Focus first on the TCE–water and 0.3% SDS–TCE–water systems, where TCE concentration was about 800–900 and 1100 mg/l, respectively. At lower Reynolds number, i.e., below 50, the flux of TCE is almost comparable between the two systems, the difference between them is only 6%; however, as Reynolds number was increased, the difference becomes significant: the flux for TCE–water system was about twice that of the TCE–SDS–water system. This reduction is due to the presence of the surfactant in the system. A certain part of the solute remains encapsulated in the core of the micelles and unavailable to the membrane in the free state. Although, TCE permeation was enhanced by higher channel velocities which correspond to higher Reynolds number, however, the non-linear part of the flux reflects the fact that the membrane transport was the limiting factor [17–19]. Due to much higher solute concentration available at higher Reynolds numbers, solute depletion is not probably important at all. For the 1% SDS–water system, TCE concentration was 3500 mg/l, which is about three times that of 0.3% SDS–water system and seven times that of TCE–water system. A linear correlation was obtained for the investigated Reynolds number range from 3 to 140, which is consistent with the flux profile for the other two systems at lower Reynolds numbers where a linear correlation was obtained as well.

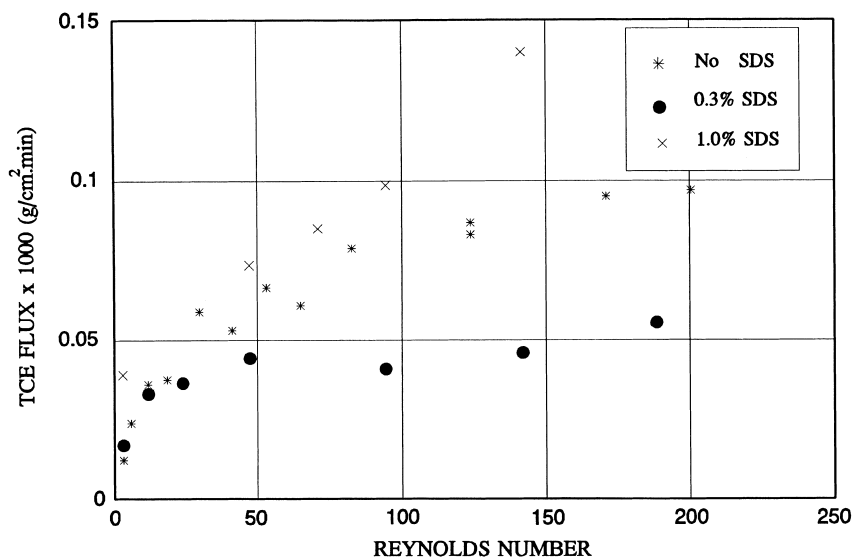


Fig. 9. Effect of hydrodynamics on TCE flux (temperature=25°C; vacuum=20 Torr; TCE=700–3500 ppm; feed-bleed mode).

4.4.4. Water flux

In pervaporation of dilute organic streams, the boundary layer mass transfer resistance for water transport is assumed to be negligible; water flux is basically a function of the water vapor pressure at the process temperature and water permeability, if the downstream

pressure is negligible and the membrane water permeability is constant. Then, water flux should be affected by temperature only. The results of water flux versus Reynolds number are shown in Fig. 10. Water flux was independent of the feed flow rate, which is analogous to that in the TCE–water system [11].

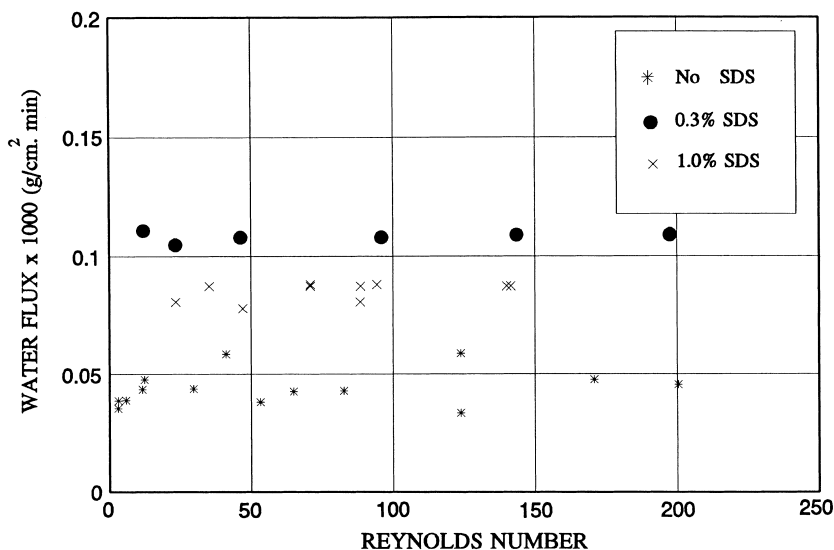


Fig. 10. Effect of hydrodynamics on water flux (temperature=25°C; vacuum=20 Torr; TCE=700–3500 ppm; feed-bleed mode).

4.5. Wetting of hydrophobic membranes by SDS solutions

It is well established in surface chemistry that when a drop of liquid is brought into contact with a flat solid surface, the final shape taken up by the drop depends on the relative magnitudes of molecular forces that exist within the liquid (cohesive) and between the liquid and solid (adhesive). The index of this effect is the contact angle which the liquid forms with the solid. It is generally found that liquids with low surface tension easily wet most solid surfaces giving a zero angle. Surfactants are usually used to bring down the surface tension, and thus, the contact angle. However, any surfactant solution can wet a solid surface if and only if the surface tension of the solution is equal to or lower than the critical surface tension of the solid surface [20]. It is also possible to wet the pores of a hydrophobic membrane by increasing the liquid pressure to a level that exceeds the pore wetting pressure. However, in this case, due to the presence of the non-porous silicone coating on the other side, the pore pressure is the same as that of the liquid.

When a surfactant solution of SDS present above the CMC level flows through the tube side of the hollow fiber membrane module, the aqueous solution does not wet the substrate because the surface tension of ultrapure SDS solution above CMC is about 38–40 mN/m [21–23], whereas the critical surface tension of the polypropylene substrate of Celgard X-10[®] is equal to 35 mN/m [24]. We have experimentally verified it; indeed, the porous substrate was not wetted with 0.3% SDS solution; however, it was wetted within the range $0.3% < C_{\text{SDS}} < 1.0%$. Now, above the CMC level of the surfactant, 0.24%, the surface tension of the solution should be constant, since only the free monomeric surface active agent will contribute to the reduction of the surface tension of a solution. The surface tension of SDS solution should be equal to 38–40 mN/m even at 10% SDS since above the CMC level the surfactant is only present in the form of micellar structures.

It is, however, well documented in the literature that the presence of impurities in surfactant solutions can have far reaching impact on the dynamic surface tension of ionic surfactant solutions. For a hydrophobic porous surface to be wetted by an aqueous solution, a monolayer film of surfactant molecules has to

be created by the adsorbing species on the pores leading to the artificial hydrophilization of the surface. Along with the surfactant molecules, impurities such as dodecanol, which is a product of SDS hydrolysis and frequently encountered in SDS–water systems [23] though in trace amounts, has very strong surface-active properties and could dramatically alter the interface properties and the surface tension of the solution. It has been reported in [23,25] that for SDS aqueous solutions, the amount of dodecanol at the surface (at saturation) is comparable to the SDS amount even in the presence of added salts [26]. Finally, the presence of surface active impurities is a decisive factor capable of lowering the surface tension of SDS solution by 2–4 mN/m than the theoretical, and particularly, at higher SDS concentrations where the rate of surfactant hydrolysis is higher, which ultimately results in higher production of impurities, and consequently, lower surface tension.

4.5.1. Wetted pore experiments

When a surfactant solution having a surface tension lower than the critical surface tension of the porous substrate flows through the lumen side of the hollow fibers, it wets the pores of the substrate; the pores are filled with the feed solution as compared to being air-filled (as in stripmeation). To estimate the resistance offered by the wetted pore, experiments were conducted with the pores of the non porous silicone coated polypropylene hollow fiber substrate deliberately filled with water. The temperature was 25°C and a vacuum of 20 Torr was maintained. Feed flow was on the tube side. The results are expected to answer the following questions. At what surfactant concentration is the feed solution wetting the pores? What is the resistance due to the water-filled pore? Are there additional resistances? The experiments were performed in two phases. In the first phase, an aqueous solution of TCE was used as the feed. In the second phase, a surfactant solution containing TCE was used as the feed.

4.5.1.1. TCE–water system

4.5.1.1.1. Effect of feed concentration. Experiments were performed at a constant flow rate of 2.5 ml/min. TCE concentration was varied between 350 and 960 ppm. The experimental results are shown

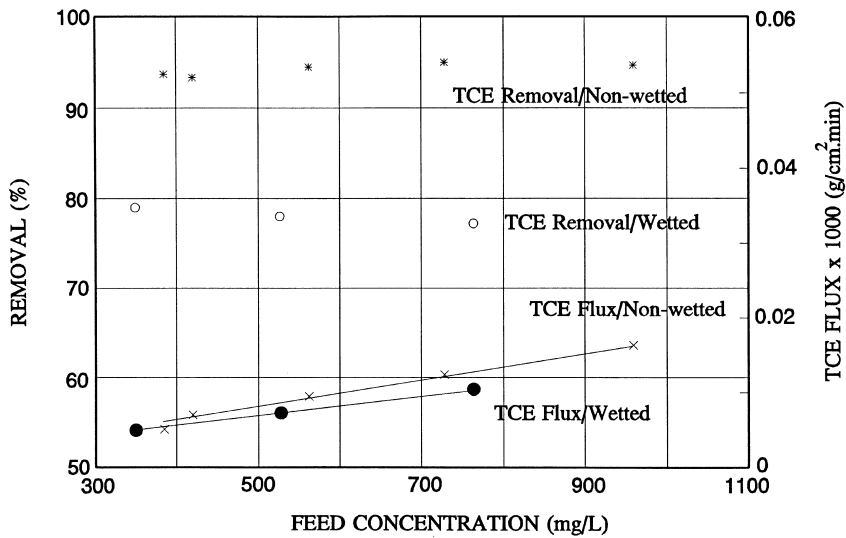


Fig. 11. TCE removal and TCE flux in experiments with wetted pore (temperature=25°C; vacuum=20 Torr; flow rate=2.5 ml/min; TCE=350–960 ppm; feed-bleed mode).

in Figs. 11 and 12. Results from stripmeation (non-wetted pores) have also been plotted for the sake of comparison. TCE removal (Fig. 11) seems to be reasonably constant and has an average value of 78%. This is significantly lower than the average TCE removal (93%) for stripmeation experiments. TCE

flux shows a similar trend. The TCE overall mass transfer coefficient (Fig. 12) for experiments with wetted pores has an average value of 4.8×10^{-4} cm/s, which is 40% lower compared to the TCE overall mass transfer coefficient for stripmeation experiments. These results are expected as the water-filled

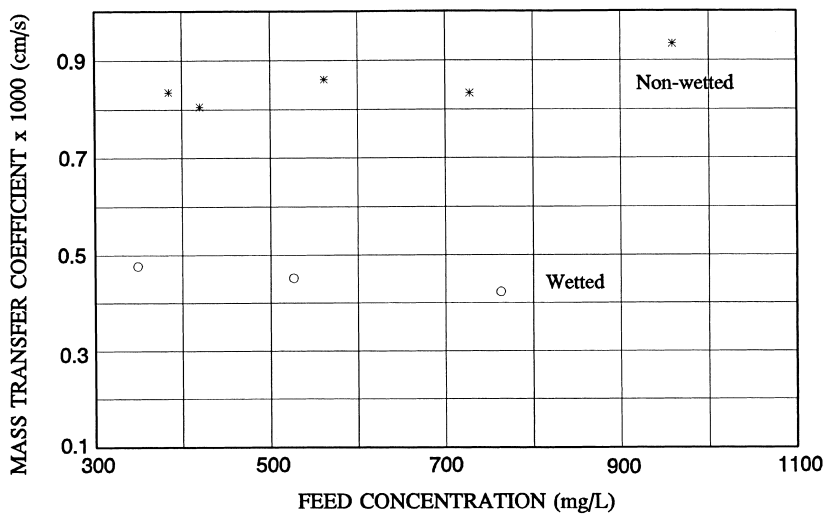


Fig. 12. TCE mass transfer coefficient in experiments with wetted pore (temperature=25°C; vacuum=20 Torr; flow rate=2.5 ml/min; TCE=350–960 ppm; feed-bleed mode).

Table 2

Experimental results comparing the effect of hydrodynamics on TCE removal, flux and mass transfer coefficient in non-wetted and wetted pores using aqueous solution of TCE as feed (temperature=25°C; vacuum=20 Torr; TCE=700–900 ppm; feed-bleed mode)

Flow rate (ml/min)	TCE removal (%)		TCE flux×1000 (g/cm ² min)		TCE mass transfer coefficient×1000 (cm/s)	
	Non-wetted	Wetted	Non-wetted	Wetted	Non-wetted	Wetted
10	58	36	0.027	0.021	1.1	0.5
25	45	18	0.059	0.024	1.4	0.55
35	37	15	0.065	0.031	1.5	0.65

pores of the substrate offers an additional resistance to the transport of TCE across the hollow fiber. This resistance is now estimated as follows.

For experiments with wetted pore, the overall mass transfer coefficient, K_o , may be obtained from Eq. (12). The overall mass transfer coefficient for stripmeation experiments is given by Eq. (13) and written here as

$$\frac{1}{K_{o_{\text{non-wet}}}} = \frac{d_o}{d_i} \frac{1}{k_1^f} + \frac{H_{ig}}{m_{vf} k_m} \quad (23)$$

The feed side boundary layer mass transfer coefficient, k_1^f , and the membrane resistance, k_m , may be assumed to be similar for both cases. Further m_{vf}/H_{ig} and m_{vf}/H_{il} may be assumed to be identical at low TCE concentrations. Also, H_{il} in Eq. (12) may be assumed to be unity, as pores are water-filled and there is no striping. Subtracting Eq. (23) from Eq. (12), Eq. (24) is obtained:

$$\frac{1}{K_o} = \frac{1}{K_{o_{\text{non-wet}}}} + \frac{d_o}{d_{lm} k_{ip}^f} \quad (24)$$

Substituting from Fig. 12, $K_o=4.8 \times 10^{-4}$ cm/s, $K_{o_{\text{non-wet}}}=8.6 \times 10^{-4}$ cm/s, $d_o=290 \times 10^{-4}$ cm and $d_{lm}=264 \times 10^{-4}$ cm, k_{ip}^f is obtained as 1.18×10^{-3} cm/s. The value of k_{ip}^f , the TCE mass transfer coefficient in the water-filled pore, is comparable to $K_{o_{\text{non-wet}}}$ and cannot be ignored. Therefore, when conditions are such that the surfactant feed wets the pores, the resistance offered by the water-filled pores is one of the contributing resistances that lowers the TCE flux across the hollow fiber.

4.5.1.1.2. Effect of feed flow rate. In the previous section the value of k_{ip}^f has been calculated. Conceptually, the value of k_{ip}^f should be similar for any feed flow rate. Therefore, experiments were

carried out at different feed flow rates. The pores of the hollow fiber membrane module were kept water-filled. The experiments were conducted at three flow rates: 10, 25 and 35 ml/min. TCE concentration was maintained between 700 and 900 ppm. Table 2 illustrates TCE removal and TCE flux behavior. Table 2 also has the TCE overall mass transfer coefficient for wetted and non-wetted pores. TCE removal (Table 2) changes from 36% to 15% as the flow rate was changed from 10 to 35 ml/min. TCE flux shows a steady increase with an increase in the feed flow rate. The overall TCE mass transfer coefficient also increases with increasing flow rate. It is evident that TCE removal, TCE flux and TCE overall mass transfer coefficient have lower values compared to stripmeation experiments and this is due to the water-filled pore resistance. Using a procedure similar to that used in Section 4.5.1.1.1, k_{ip}^f was calculated for each flow rate and is listed in Table 3. It is clear that k_{ip}^f is reasonably constant with changing flow rate. Therefore, it might be assumed that the approach used for the calculation of k_{ip}^f is valid. A theoretical estimate of the water-filled pore resistance was obtained using Eq. (14).

Substituting the values of $D_{il}=9 \times 10^{-6}$ cm²/s [27], $\epsilon_m=0.4$, $\tau_m=2.5$ and $\delta_s=2.5 \times 10^{-3}$ cm [28], the mass transfer coefficient of TCE in a water-filled pore, k_{ip}^f , is calculated to be 5.76×10^{-4} cm/s. It is evident that the theoretically calculated value of k_{ip}^f is lower than that obtained experimentally, i.e., the theoretical estimate of the resistance to transport of TCE across a water-filled pore is higher. The difference may be due to a monolayer of TCE adsorbed on the wall of the pores of the substrate. This layer would then facilitate the transport of TCE by allowing surface diffusion of TCE along the walls of the substrate, from the bulk solution to the silicone skin.

Table 3

Experimental and calculated results to determine water-filled pore resistance (TCE–water system; temperature=25°C; vacuum=20 Torr; once-through mode)

Flow rate (ml/min)	Feed concentration (ppm)	Retentate concentration (ppm)	Removal (%)	K_{owet} (cm/s)	K_{o} (cm/s)	k_{ip}^f (cm/s)
10	807	517	36	0.001	0.0011	0.001
25	785	648	17.4	0.001	0.0014	0.001
35	812	690	15	0.001	0.0015	0.0012

4.5.2. TCE–water–SDS system

4.5.2.1. Effect of surfactant concentration. This section discusses results from experiments performed using a surfactant solution containing TCE as feed. The feed solution was passed through the bore of the hollow fibers having wetted pores at a flow rate of 2.5 ml/min. Two surfactant concentrations were used: 0.3% and 1%. For 0.3% SDS, TCE concentration was varied between 300 and 800 ppm. For 1% SDS, TCE concentration was varied in the range 700–2600 ppm. Figs. 13–15 illustrate the behavior of TCE removal, TCE flux and TCE mass transfer coefficient, respectively. In all figures, the corresponding results from non-wetted pore experiments have also been plotted. TCE removal

for 0.3% SDS has an average value of 78%, which is significantly lower than that for non-wetted pore (86%). For 1% SDS, the value for TCE removal is similar for wetted and non-wetted cases. From the above results it may be inferred that the pores are not wetted at 0.3% SDS and the lower removal with wetted pores is due to the resistance offered by the water-filled pore. Further, the results indicate that at 1.0% SDS concentration, the pores are wetted. TCE flux (Fig. 14) for 0.3% SDS (wetted) is, as expected, lower than 0.3% SDS (non-wetted). TCE fluxes for wetted and non-wetted modes of operation at 1.0% SDS are comparable to each other. Similar behavior is observed for the TCE overall mass transfer coefficient. For 0.3% SDS (wetted), the TCE overall mass transfer coefficient is 4.8×10^{-4} cm/s compared to $6.5 \times$

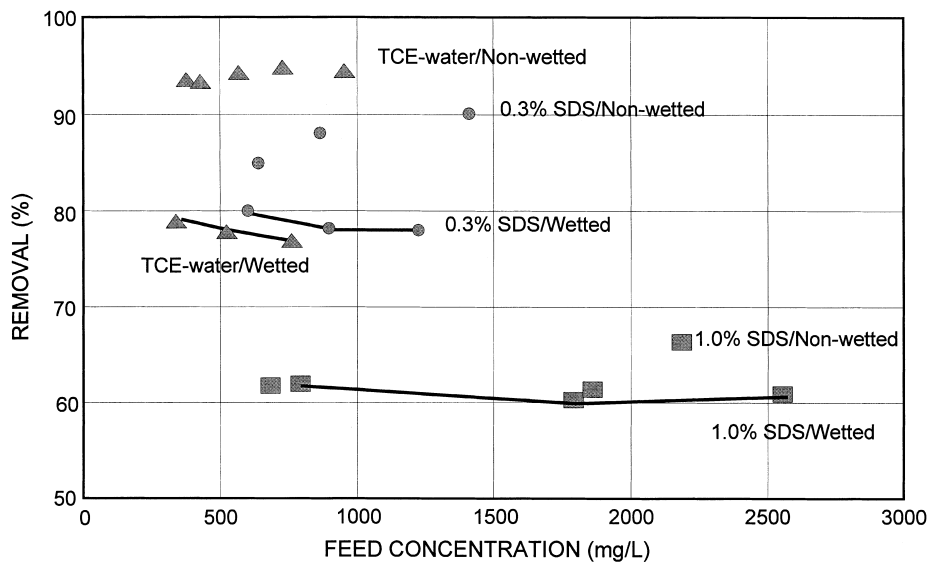


Fig. 13. Removal of TCE in wetted versus non-wetted pore (temperature=25°C; vacuum=20 Torr; flow rate=2.5 ml/min; once-through mode).

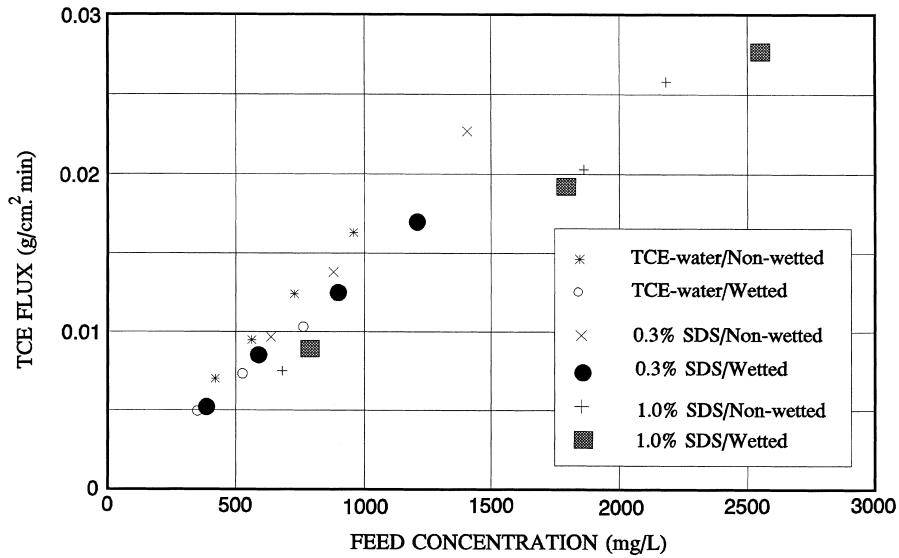


Fig. 14. Effect of surfactant concentration on TCE flux in experiments with wetted pore (temperature=25°C; vacuum=20 Torr; flow rate=2.5 ml/min; once-through mode).

10^{-4} cm/s for the non-wetted system. At 1.0% SDS the overall TCE mass transfer coefficient for the two modes of operation are similar.

We can now carry out a calculation similar to that for the TCE–water system via Eq. (24). For 0.3% SDS system, the values for K_o and $K_{o_{\text{non-wet}}}$ are 4.622×10^{-4}

and 6.345×10^{-4} cm/s, respectively. From Eq. (24), we can obtain $k_{\text{ip}}^f = 1.868 \times 10^{-3}$ cm/s. The value of k_{ip}^f obtained from Eq. (14) is equal to 0.576×10^{-3} cm/s. Comparing both values it can be noticed that mass transfer resistance estimated according to Eq. (24) is about three times lower than that obtained

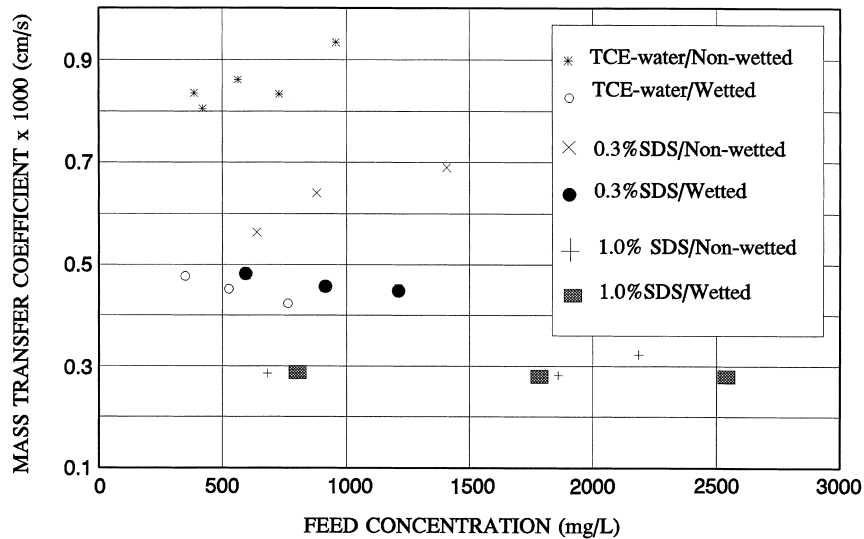


Fig. 15. Effect of surfactant concentration on TCE mass transfer coefficient in experiments with wetted pore (temperature=25°C; vacuum=20 Torr; flow rate=2.5 ml/min; once-through mode).

from Eq. (14), i.e., the theoretical estimate of the water-filled pore resistance. Why?

4.5.2.2. TCE mass transfer and micellar transport. The previous theoretical considerations assumed TCE–SDS–water system as a homogeneous system; however, due to the presence of microstructures, it is rather a pseudo-homogeneous system. Therefore, the discrepancy found earlier may be attributed to the presence of micellar microstructures where almost all of the TCE is solubilized in the micellar core (TCE distribution coefficient between the micelles and extra-micellar environment is about 1900 [29]). This means that most of the TCE is present in the micellar core. The concentration of micelles for 0.3% SDS will be about 3.69572×10^{-5} M, assuming that the aggregation number for this range of SDS concentration is equal to 65 [16] and the CMC is 8×10^{-3} M. The concentration of TCE is about 1000 ppm which is equal to 7.6109×10^{-3} M. The molar ratio of TCE/micelle is equal to 206. In other words, there are about 206 molecules of TCE per micelle. Every effective disintegration of the micelle will result in a huge amount of TCE released as micellar diffusion occurs in the pore. The diffusion coefficient of a spherical micelle consisting of 65 monomers was estimated from Stokes–Einstein equation

$$D_m = \frac{kT}{6\pi\eta r_H} \quad (25)$$

and was found to be equal to 1.25×10^{-6} cm²/s, which is about seven times lower than the TCE diffusion coefficient in water. The radius of a spherical micelle was estimated from Tanford's equation by estimating the volume of the hydrocarbon chain of the surfactant

which makes up the core of the micelle from

$$V_m = N_m(27.4 + 26.9nC') \times 10^{-3} \text{ (nm}^3\text{)} \quad (26)$$

(where N_m is the aggregation number and C' is the number of carbon atoms in the hydrocarbon chain minus one). Therefore, the difference between the theoretical value of k_{lp}^f and the one estimated from the model (wetted case) can be attributed to the enhanced micellar transport of TCE in the wetted porous substrate of the hollow fiber. Additional evidence of such unusual enhancement in TCE mass transfer is the gradual increase in TCE mass transfer coefficient versus concentration (see Fig. 6). The micelles here are acting as a mobile vehicle containing substantial amount of TCE and supplying it to the membrane. At this stage, it is difficult to predict exactly the micellar contribution to TCE mass transfer in the absence of structural data.

4.5.2.3. Effect of feed flow rate. Experiments were performed using 0.3% SDS feed solution at different feed flow rates. TCE concentration was varied between 1100 and 1200 ppm. Experiments were carried out at four flow rates: 2.5, 10, 20 and 40 ml/min. The results are shown in Table 4. It is evident that TCE removal and TCE flux are lower for experiments with wetted pore. TCE removal dropped from 79% to 10% as the flow rate was increased from 2.5 to 40 ml/min. TCE overall mass transfer coefficient is almost constant with changing feed flow rate. It has an average value of 5.0×10^{-4} cm/s compared to 6.45×10^{-4} cm/s for non-wetted pores. The above results corroborate the fact that at 0.3% SDS the feed solution does not wet the pores.

From Sections 4.5.2.1 and 4.5.2.2 it may be inferred that the pores are wetted somewhere between 0.3%

Table 4

Experimental results comparing the effect of hydrodynamics on TCE removal, flux and mass transfer coefficient in non-wetted and wetted pores using surfactant solution of TCE as feed (SDS=0.3% SDS; temperature=25°C; vacuum=20 Torr; TCE=1000–1100 ppm; feed-bleed mode)

Flow rate (ml/min)	TCE removal (%)		TCE flux $\times 1000$ (g/cm ² min)		TCE mass transfer coefficient $\times 1000$ (cm/s)	
	Non-wetted	Wetted	Non-wetted	Wetted	Non-wetted	Wetted
2.5	90	79	0.017	0.015	0.65	0.45
10	44	37	0.034	0.029	0.64	0.54
20	25	20	0.037	0.031	0.64	0.48
40	17	10	0.049	0.029	0.65	0.50

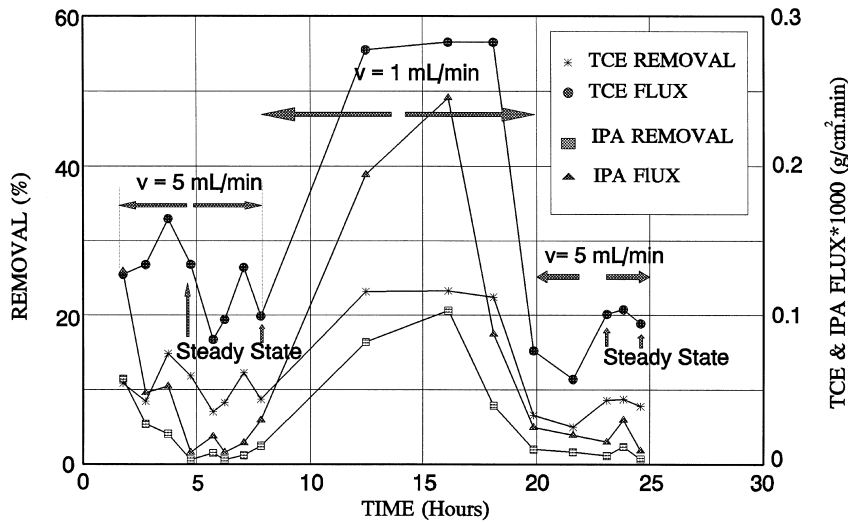


Fig. 16. Removal of TCE in the presence of a hydrophilic polymer and isopropanol (temperature=25°C; 4% SDS; 4% IPA; TCE=7000 ppm; xanthan gum=250 ppm).

SDS and 1.0% SDS concentration. As discussed earlier, the controlling resistances for TCE–water system are the feed-side boundary layer resistance and the membrane resistance. For surfactant system, there are two additional resistances that impede the transport of TCE. One is the water-filled pore resistance, which is applicable only under conditions when the surfactant solution wets the pore. The other is the resistance offered by surfactant micelles to release free TCE. The TCE molecules are encapsulated in the micellar core and are not available in the bulk. As the surfactant concentration increases, the probability of a micelle colliding with the wall and releasing TCE decreases. Therefore, the availability of free TCE in the system is limited. Hence, as the surfactant concentration increases, there is a steady drop in the TCE overall mass transfer coefficient.

4.6. Removal of VOCs from surfactant-flushed water containing polymers and alcohol

We have also investigated and studied the efficacy and suitability of the hollow fiber membrane-based modified pervaporation process for the treatment of specific remediated site groundwater. In this particular case, apart from TCE, the feed contained: 4% SDS; 4% isopropyl alcohol (IPA) and 200 ppm hydrophilic polymer xanthan gum. The latter two components are

used to enhance the performance of the middle phase (microemulsion), increase the viscosity of the micellar system, and thus, the capillary number which in turn enhances the wetting phenomenon in the soil porous structure, and obviously, increasing the solubilization of VOCs in the micellar phase.

Fig. 16 represents the removal of IPA and TCE versus time. The purpose of this 25 h run was to study the performance of the hollow fiber module over an extended period. The flow rate was varied from 5 to 1 ml/min overnight. During this period no change in the flux of IPA and TCE was observed. The module performance at hour 6–9 was identical to that at hour 22–24. The removal of TCE and IPA was sustained at the same level of 20–23% and 2–3%, respectively. The huge peaks in the middle of the chart correspond to the night shift when the feed flow rate was intentionally reduced, and consequently, resulted in a higher removal of TCE and IPA due to the higher residence time.

5. Concluding remarks

In the present study, we have shown the feasibility of the hollow fiber membrane-based pervaporation process to handle a variety of streams, namely, TCE–water, TCE–SDS–water and TCE–SDS–IPA–

xanthan gum–water aqueous solutions. Efficient removal of VOC from such solutions was shown to be achievable. Mass transfer coefficient of TCE is primarily controlled by the feed boundary layer and membrane resistances for non-wetted pore case, and by pore diffusion resistance for wetted pore case. The presence of surfactants such as SDS in the aqueous solution affects TCE mass transfer coefficient; the higher the surfactant concentration, the lower the mass transfer coefficient. This impact can be minimized by maximizing the molar ratio of solute/surfactant as seen in Fig. 6 for 0.3% SDS system. It is yet unclear what is the exact mechanism of mass transfer of TCE from the core of the micellar structure to the membrane. The resistances-in-series concept was found to be adequate to explain the TCE–water system [11] mass transfer both for wetted and non-wetted pores. To describe the transfer in TCE–SDS–water system, the mechanism of effective TCE mass transfer to the membrane in a micellar environment has to be developed quantitatively.

6. Notation

A_m	membrane area based on fiber outside diameter (cm^2)	C''_{imp}	concentration of species i in the vacuum side at the silicone membrane–vacuum side interface (g mol/cm^3)
C'	number of carbon atoms in hydrocarbon chain of surfactant minus unity	C''_{ip}	bulk concentration of species i in the vacuum side (g mol/cm^3)
C'_{il}	bulk liquid phase feed concentration of species i (g mol/cm^3)	C''_{ipl}	hypothetical equilibrium liquid phase concentration in equilibrium with the vacuum side gas phase, $C''_{ipl} = H_{ig} C''_{ip}$ (g mol/cm^3)
C'_i, C'_j	feed concentration of species i and j , respectively (g mol/cm^3)	C'_{ilpi}	liquid phase concentration of solute i in the pore in equilibrium with the bulk phase feed concentration of species i (g mol/cm^3)
C'_{ili}	concentration of species i in the aqueous feed phase at the aqueous–pore gas interface (g mol/cm^3)	C'_{ilpmi}	concentration of species i in the liquid phase in the pore at the aqueous–silicone membrane interface (g mol/cm^3)
C'_{igi}	concentration of species i in the vapor phase at the aqueous–pore gas interface (g mol/cm^3)	C_{inlet}	feed aqueous inlet concentration of TCE (g mol/cm^3)
C'_{igmi}	concentration of species i in the vapor phase at the pore gas–silicone membrane interface (g mol/cm^3)	C_{outlet}	feed aqueous outlet concentration of TCE (g mol/cm^3)
C'_{imi}	concentration of species i in the membrane at the pore gas–silicone membrane interface (g mol/cm^3)	C^p_{inlet}	hypothetical permeate aqueous concentration of TCE at feed inlet location in equilibrium with the vacuum phase (g mol/cm^3)
C''_{imi}	concentration of species i in the membrane at the silicone membrane–vacuum side interface (g mol/cm^3)	C^p_{outlet}	hypothetical permeate aqueous concentration of TCE at feed outlet location in equilibrium with the vacuum phase (g mol/cm^3)
		ΔC_{Im}	logarithmic mean aqueous concentration of TCE as defined by Eq. (22) (g mol/cm^3)
		d_i	inner diameter of Celgard hollow fiber (cm)
		d_o	outer diameter of Celgard hollow fiber (cm)
		d_{lm}	logarithmic mean diameter of Celgard hollow fiber, $(d_o - d_i) / \ln(d_o / d_i)$
		D_m	diffusion coefficient of micelles (cm^2/s)
		D_{igp}	diffusion coefficient of TCE in the gaseous pore (cm^2/s)
		D_{il}	diffusion coefficient of TCE in water (cm^2/s)
		D_{iwp}	diffusion coefficient of TCE in water in the pore, D_{il} (cm^2/s)
		H_{ig}	Henry's law constant for species i defined by Eq. (2a) $(\text{mg/l})_{liq} / (\text{mg/l})_{vap}$
		J_i	permeation flux of species i ($\text{g/cm}^2 \text{sec}$)
		J_w	permeation flux of water ($\text{g/cm}^2 \text{sec}$)

K_o	overall mass transfer coefficient defined by Eq. (21) (cm/s)
$K_{o_{\text{non-wet}}}$	overall mass transfer coefficient for non-wetted pore defined by Eq. (23) (cm/s)
k	Boltzmann constant (J/K)
k_g^p	vacuum-side mass transfer coefficient (cm/s)
k_{gp}^f	mass transfer coefficient for mass transfer across the gas-filled pore (cm/s)
k_{lp}^f	theoretical mass transfer coefficient for mass transfer across the aqueous-filled pore (cm/s)
k_l^f	aqueous phase mass transfer coefficient for mass transfer across the feed-side boundary layer (cm/s)
k_m	mass transfer coefficient for mass transfer across the membrane (cm/s)
L	active length of the module (cm)
m_{vp}	distribution coefficient of TCE between the vacuum side and the membrane
m_{vf}	distribution coefficient of TCE between the membrane and the gaseous phase
M_i	molecular weight of species i
n	number of hydrocarbon chains in a surfactant molecule
N	number of hollow fibers
N_m	aggregation number of a micelle
Q	volumetric liquid flow rate (cm ³ /min)
r_H	hydrodynamic radius of micelles (m)
r_i	radius of a tube (cm)
R	gas constant, 8.31441 (J/mol K)
R_i	permeation rate of species i per unit permeator length (g mol/cm s)
Re	Reynolds number as defined by Eq. (19)
t	time (s)
T	temperature (K)
v	linear velocity of the feed (cm/s)
V_m	volume of micelle (nm ³)
V_{TCE}	volume of TCE collected (cm ³)
V_{H_2O}	volume of water collected (cm ³)

Greek symbols

δ_m	fiber substrate thickness (cm)
ϵ_m	porosity of the Celgard X-10 fibers for use in Eq. (14)
τ_m	tortuosity of pores in the Celgard X-10 fibers and equal to 2.49

π	3.1416
η	dynamic viscosity of water in Eq. (18)
ρ_{H_2O}	density of water and equal to 1 g/cm ³
ρ_{TCE}	density of TCE, 1.456 g/cm ³
μ_{H_2O}	viscosity of water, 0.001 g/cm s

Acknowledgements

This research was conducted under the SERDP (Strategic Environmental Research and Development Program) project, EPA-371-94, administered through the EPA Northeast Hazardous Substance Research Center at Newark, NJ 07102. The supply of coated hollow fibers by AMT is gratefully acknowledged.

References

- [1] D.A. Sabatini, R.C. Knox, J.H. Harwell, Emerging technologies in surfactant-enhanced subsurface remediation, in: D.A. Sabatini, R.C. Knox, J.H. Harwell (Eds.), *Surfactant Enhanced Subsurface Remediation, Emerging Technologies*, ACS Symposium Series, vol. 594, 1995, pp. 1–8.
- [2] J.H. Nash, Field studies of in situ soil washing, US Environmental Protection Agency, Washington, DC 20460, EPA/600/2-85/129, 1986.
- [3] J.C. Fountain, Field test of surfactant flooding: mobility control of dense non-aqueous phase liquids, ACS Sympo. Ser. 491 (1992) 182–191.
- [4] C.C. West, J.H. Harwell, Surfactants and subsurface remediation, *Environ. Sci. Technol.* 26 (1992) 2324.
- [5] J.C. Fountain, C. Waddel-Sheets, A. Lagowski, C. Taylor, D. Frazier, M. Byrne, Enhanced removal of DNAPLs using surfactants, ACS Symp. Ser. 594 (1995) 177–190.
- [6] G.M. Long, Clean up hydrocarbon contamination effectively, *Chem. Eng. Prog.* 89(5) (1993) 58.
- [7] Jian-Shen Jiang, L.M. Vane, S.K. Sikdar, Recovery of VOCs from surfactant solutions by pervaporation, *J. Membr. Sci.* 136 (1997) 233.
- [8] L. Vane, F. Alvarez, L. Hitchens, J. Burckle, L. Yeh, Separation of VOCs from surfactant-enhanced aquifer remediation fluid using pervaporation, in: *Proceedings of the Ninth Annual Meeting of North American Membrane Society*, F5, Baltimore, 1997.
- [9] I. Abou-Nemeh, A. Das, S. Chandra, A. Saraf, K.K. Sirkar, Removal of VOCs from surfactant-flushed water by a novel hollow fiber membrane based pervaporation process, *Preprints of Topical Conference on Separation Science and Technology, Annual Meeting of AIChE*, vol. 1, 1997, pp. 695–700.
- [10] I. Abou-Nemeh, A. Das, S. Chandra, A. Saraf, K.K. Sirkar, Removal of VOCs from surfactant-flushed water by a novel hollow fiber membrane based pervaporation process, *Proceedings of the 10th Annual Meeting of the North American Membrane Society*, Cleveland, 1998, 33.

- [11] A. Das, I. Abou-Nemeh, S. Chandra, K.K. Sirkar, Membrane-moderated stripping process for removing VOCs from water in a composite hollow fiber module, *J. Membr. Sci.* 148(2) (1998) 257.
- [12] S. Chandra, Removal of volatile organic compounds from contaminated groundwater by pervaporation, M.S. Thesis, New Jersey Institute of Technology, Newark, New Jersey, 1996.
- [13] M. Markelov, J.P. Guzowski Jr., Matrix independent head-space gas chromatographic analysis. The full evaporation technique, *Anal. Chim. Acta* 15 (1993) 234.
- [14] R.R. Bhawe, K.K. Sirkar, Gas permeation and separation by aqueous membranes immobilized across the whole thickness or in a thin section of hydrophobic microporous Celgard films, *J. Membr. Sci.* 27 (1986) 41.
- [15] D.T. Leighton, J.M. Calo, Distribution coefficients of chlorinated hydrocarbons in dilute air–water systems for ground water contamination applications, *J. Chem. Eng. Data* 26(4) (1981) 382.
- [16] R.P. Robertson, D.J. Wilson, Soil cleanup by in situ surfactant flushing. IX. Electrical effects in micelle formation, *Sep. Sci. Technol.* 30(14) (1995) 2821.
- [17] K. Psaume, P. Aptel, Y. Aurelle, J.C. Mora, J.L. Bersillon, Pervaporation: importance of concentration polarization in the extraction of trace organics from water, *J. Membr. Sci.* 36 (1988) 373.
- [18] J.G. Wijmans, A.L. Athayde, R. Daniels, J.H. Ly, D. Kamaruddin, I. Pinnau, The role of boundary layers in the removal of volatile organic compounds from water by pervaporation, *J. Membr. Sci.* 109 (1996) 135.
- [19] X. Feng, R.Y.M. Huang, Liquid separation by membrane pervaporation. A review, *Ind. Eng. Chem. Res.* 36 (1997) 1048.
- [20] E.G. Shafrin, W.A. Zisman, Upper limits to contact angles of liquids on solid, in: *Contact Angle, Wettability and Adhesion*, Advances in Chemistry Series, vol. 43, ACS Applied Publications, 1964, 145 pp.
- [21] K. Tajima, Radiotracer studies on adsorption of surface active substance at aqueous surface. II. The effect of excess salt on the adsorption of sodium dodecylsulfate, *Bull. Chem. Soc. Jpn.* 43 (1970) 3063.
- [22] W. Brown, J. Zhao, Adsorption of sodium dodecylsulfate on polystyrene latex particles using dynamic light scattering and zeta potential measurements, *Macromolecules* 26 (1993) 2711.
- [23] A. Bonfillon, F. Sicoli, D. Langevin, Dynamic surface tension of ionic surfactant solutions, *J. Colloid Interface Sci.* 168 (1994) 497.
- [24] Celgard microporous polypropylene film, Technical information by Celanese, 1980.
- [25] K.J. Mysels, R.E. Stafford, Time and concentration resolved surface tension, *Colloids Surf.* 51(23) (1990) 105.
- [26] E.J. Staples, L. Thompson, I. Tucker, J. Penfold, Effect of dodecanol on mixed nonionic and nonionic/anionic surfactant adsorption at air/water interfaces, *Langmuir* 10(11) (1994) 4136.
- [27] C. Lipski, P. Cote, The use of pervaporation for the removal of organic contaminants from water, *Environ. Prog.* 9 (1990) 254.
- [28] R. Prasad, K.K. Sirkar, Dispersion free solvent extraction with microporous hollow fiber modules, *AIChE J.* 34 (1988) 177.
- [29] B. Shaiu, J.D. Rouse, D.A. Sabitini, J.H. Harwell, Surfactant selection for optimizing surfactant-enhanced subsurface remediation, *ACS Symp. Ser.* 594 (1995) 65.